

Limnol. Oceanogr., 41(1), 1996, 182–189
© 1996, by the American Society of Limnology and Oceanography, Inc.

Calculation of cell-specific growth rates: A clarification

Abstract—Cell-specific growth and cell-specific production estimates of phytoplankton have been calculated in the past by a simple exponential model (constant uptake-division) that describes the time rate of change of carbon, C^* , and assumes both continuous division and continuous carbon uptake. We propose three new models (variable uptake-division, variable uptake-constant division, and diurnal) for making more accurate estimates of the algal growth rate, μ . The variable uptake-division model is the most complex and requires species-specific information on the division pattern. The diurnal model can provide accurate μ estimates while requiring only two measurements of C^* and no other parameters, but it requires 48-h incubation times. The variable uptake-constant division model can also provide accurate μ estimates and can be applied to data with <24-h incubation times. The variable uptake-division and variable uptake-constant division models require additional work compared to the constant uptake-division model, but the effort is warranted because they also provide a direct approach for quantifying the dependence of μ on the photoperiod and thus enable greater confidence in applying μ to ecological studies, in which the light climate may differ from that of the experiment.

During the past 20 yr, several investigators have measured cell-specific phytoplankton production with techniques such as autoradiography and sorting of individual cells with liquid scintillation counting (Knoechel and Kalff 1976; Rivkin and Seliger 1981; Subba Rao 1988). These cell-specific production values have been used to estimate species-specific growth rates that have provided important insights into individual population dynamics and the factors controlling phytoplankton succession (Knoechel and Kalff 1975, 1978). However, these species-specific techniques, particularly autoradiography, are tedious and time-consuming, which prevents their widespread application. With the advent of flow cytometry, it is possible to make cell-specific measurements in a more timely fashion, and it is likely that more of these measurements will be made in the near future (Rivkin et al. 1986; Li 1994). Our purpose here is to provide a more accurate method for estimating cell-specific growth rates from cell-specific carbon uptake. Cell-specific growth rates are the rates at which the cell biomass or carbon increases, which is distinct from the cell division process. Cell-specific carbon uptake estimates commonly have been based on incubations of variable length (usually <24 h) and have not addressed the potential errors caused by assuming that carbon uptake and cell division are continuous processes.

At the cellular level, the time rate of carbon change can be described as

$$\frac{dC^*}{dt} = \alpha U - \mu C^* \quad (1)$$

All of the mathematical symbols used in the various models are described in the list of notation. Note that in Eq. 1 carbon production due to cell growth is always positive when viewed at the population level; however, when growth is viewed at the cellular level, carbon uptake is negative, reflecting the loss of carbon due to cell division. Furthermore, carbon loss due to cell division can only be described as a first-order rate process if the averaged response of a suitable number of cells that characterize the general species behavior is considered. The solution to Eq. 1 is straightforward, i.e.

$$C^*(t) = \frac{\alpha U}{\mu} [1 - \exp(-\mu t)]$$

$$\mu = -\frac{1}{t} \ln \left[1 - \frac{C^*(t)}{\alpha U / \mu} \right] \quad (2)$$

Equation 2 has been used to calculate the growth rate, μ , from measures of species-specific carbon uptake (Welschmeyer and Lorenzen 1984; Knoechel and Quinn 1989; Welschmeyer et al. 1991). In practice, the asymptotic concentration of $C^*(\alpha U / \mu)$ is estimated by assuming that the product of the activity of the medium (m^*) and the cell carbon content (C_a) of the algal species under study equals the upper asymptotic concentration of C^* . We refer to Eq. 1 and 2 as the constant uptake-division model (CUDM).

Notation

| | |
|---------------------|--|
| C^* | ^{14}C (dpm cell $^{-1}$); new carbon (pg C cell $^{-1}$) in data example section |
| α | Isotope discrimination factor |
| U | Uptake rate of C^* (d $^{-1}$) |
| μ | Cell growth rate (d $^{-1}$) |
| t | Time |
| m^* | Activity of the culture medium |
| C_a | Species-specific cell carbon content |
| $\lambda_1(t)$ | Time-dependent function that controls U |
| $\lambda_2(t)$ | Time-dependent function that controls μ |
| τ, ζ | Dummy variables of integration |
| C^*_{low} | Lower asymptotic C^* ; lies on curve that would pass through all diurnal minima |
| C^*_{high} | Upper asymptotic C^* ; lies on curve that would pass through all diurnal maxima |
| t_p | Time corresponding to the end of the photoperiod |
| L_0 | Weighted average of $\lambda_1(t)$ over photoperiod t_p |
| μ_{crit} | Critical μ value |

Carbon uptake and division are not necessarily continuous processes (Soder 1966; Chisholm 1981) even when averaged over large numbers of cells; therefore, the time-course of C^* may be poorly approximated by the CUDM. Investigators who have used this model have either ig-

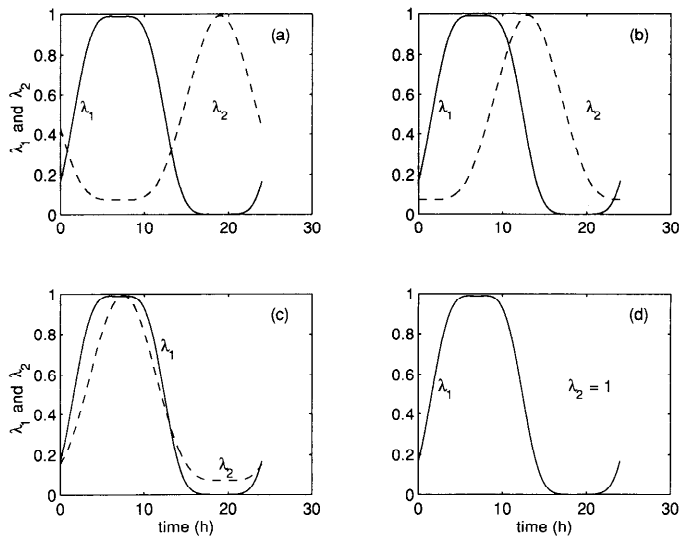


Fig. 1. Four different daily patterns for carbon uptake and growth for a 14:10 L/D cycle. The solid line describes λ_1 , the carbon uptake portion of the cycle, and is the same for all cases. The dashed line represents the growth cycle, λ_2 , and describes dark dominance in panel a, mixed light/dark dominance in panel b, light dominance in panel c, and continuous division in panel d.

nored the dark period (Knoechel and Quinn 1989), used cultures grown under a continuous 24-h light period (Welschmeyer and Lorenzen 1984), or used 24-h or longer incubations for a natural population on a L/D cycle (Welschmeyer et al. 1991). Thus, problems associated with diurnal patterns of carbon fixation and division were not considered. The CUDM describes $C^*(t)$ as an exponentially increasing function of time. Experimental data, however, strongly indicate that over the course of each 24-h period, $C^*(t)$ will show relative maxima and minima (Soder 1966; Fahnenstiel and Scavia 1987; Mingelbier et al. 1994). The diurnal maximum usually occurs near the end of the light cycle, when carbon uptake is in progress. The diurnal minimum usually occurs near the end of the dark cycle, when cell division is the dominant process. The relative difference between these maxima and minima is controlled by those processes described by Eq. 1 and by the nature of the diurnal cycle of carbon uptake and cell division. It is important to note that these models and our subsequent analyses ignore the loss of fixed carbon by respiration, exudates, etc. Instead, we focus only on describing the coupling between carbon uptake and division.

To better describe carbon uptake and cell division over the diurnal cycle, we need to account for the temporal response of these processes. Let λ_1 be a time-dependent function that ranges from zero to one and that controls carbon uptake. Correspondingly, let λ_2 be a time-dependent function that ranges from zero to one and that controls cell division. When λ_1 and λ_2 are set equal to one and held constant in time, we have the CUDM. To illustrate how λ_1 and λ_2 may be incorporated into the prob-

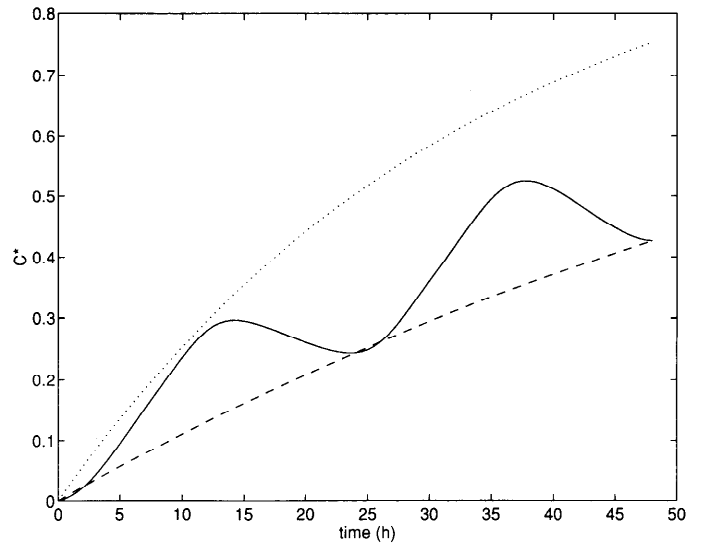


Fig. 2. The solid line is a realistic portrayal of the daily cycle of C^* seen in cell-specific data. It was generated by the variable uptake-division model. The dotted and dashed lines are exponential descriptions of C^* . The dotted line was generated by the constant uptake-division model with $\mu = 0.7 \text{ d}^{-1}$. The dashed line was generated by the diurnal model.

lem, we will assume a 14:10 L/D cycle. The carbon uptake and division cycles are represented by the plots shown in Fig. 1. Figure 1a shows cell division occurring primarily during the dark cycle. Figure 1b has cell division peak near the transition period between the light and dark cycle. In Fig. 1c, cell division is concentrated during the light cycle, and in Fig. 1d cell division is continuous throughout the light and dark cycles. Rewriting Eq. 1 to account for these effects gives us the more general problem of

$$\frac{dC^*(t)}{dt} = \lambda_1 \alpha U - \lambda_2 \mu C^*(t). \quad (3)$$

The general solution to Eq. 3 is

$$C^*(t) = \alpha U \int_0^t \lambda_1(\tau) \exp[-\mu \Lambda_2(t - \tau)] d\tau \quad (4)$$

where

$$\Lambda_2(t - \tau) = \int_{\tau}^t \lambda_2(\zeta) d\zeta. \quad (5)$$

The exponential term in the convolution integral Eq. 4 can be interpreted as a filter that moves in time and modifies production. The dummy variables of integration, τ and ζ in Eq. 4 and 5, illustrate how this filter works (i.e. C^* at time t is the time-weighted sum of all previous contributions to C^*). When this time-weighting is constant in time, Eq. 4 and 5 reduce to the CUDM.

Equations 3–5 will be referred to as the variable uptake-division model (VUDM). The solid line in Fig. 2 was calculated by this model. It was calculated by assuming

a 14:10 L/D cycle with division concentrated during the dark cycle (i.e. λ_1 and λ_2 as described by Fig. 1a). A growth rate of 0.7 d^{-1} was used, and $\alpha U/\mu$ was set equal to one. By setting $\alpha U/\mu = 1$, the scaling in the figure is simplified because the maximum calculated C^* concentration will be on the order of one for the VUDM, while it will be exactly one for the CUDM. The stair-steplike response shown by the solid line conforms to observations (Harris 1978; Fahnenstiel and Scavia 1987). However, exponential fits generated by the CUDM, like the dotted line in Fig. 2, have been used to estimate growth rates from 24-h incubations (Welschmeyer and Lorenzen 1984; Laws et al. 1987; Welschmeyer et al. 1991).

To obtain the parameters necessary for describing C^* according to the VUDM requires detailed species-specific knowledge on the division cycle of the algal cells. Are the cells continuously dividing, dividing primarily during the light or dark portion of the cycle, or dividing during some fraction of the light and dark cycle? Such questions must be answered if this model is to be applied rigorously. Under some circumstances, two simpler approaches can be developed that are useful for estimating μ .

First, when experimental data behave like the VUDM (see Fig. 2), the simplest exponential fit to that data with an analytical solution is the dashed line shown in Fig. 2. This line passes through all of the relative minima of $C^*(t)$ (which obviously occur every 24 h). By requiring the fitted line to pass through these diurnal minima, the resulting curve represents the net daily growth of C^* , which satisfies our objective. The other useful approach for estimating μ is to apply the continuously dividing cell case (Fig. 1d) of the VUDM. We will describe these two approaches for making better estimates of μ . The first approach will require two measurements of C^* at 24 and 48 h (diurnal model), and the second will require characterization of the uptake rate modification parameter, λ_1 , estimates of m^* and C_a , and at least one measurement of C^* (VUDM).

Under the diurnal model, we want to determine the smooth exponential solution that passes through each of the diurnal minima. Recall that in the CUDM, the asymptotic concentration of $C^*(\alpha U/\mu)$ is estimated in practice by assuming that the product of the activity of the medium and the cell carbon content of the algal species under study equals the upper asymptotic concentration of C^* (i.e. $\alpha U/\mu = m^*C_a$). The growth rate, μ , is then readily calculated from one additional measurement of C^* (see Eq. 2). However, under the diurnal model approach, we can no longer estimate μ from one measurement of C^* but need at least two measurements in the absence of an estimate of the lower asymptotic value of C^* .

We have two unknowns: the lower asymptotic value of C^* (see Fig. 2) and μ , which requires measurements at two different times if a solution is to be found. Let C_{low}^* be the lower asymptotic concentration of C^* ; then at times t_1 and t_2 , we have

$$\begin{aligned} C^*(t_1) &= C_{\text{low}}^*[1 - \exp(-\mu t_1)] \\ C^*(t_2) &= C_{\text{low}}^*[1 - \exp(-\mu t_2)]. \end{aligned} \quad (6)$$

After performing some elementary operations on Eq. 6, $C^*(t_2)$ can be expressed as

$$C^*(t_2) = C_{\text{low}}^* \left\{ 1 - \left[\frac{C_{\text{low}}^* - C^*(t_1)}{C_{\text{low}}^*} \right]^{t_2/t_1} \right\}. \quad (7)$$

The simplest nontrivial solution to Eq. 7 occurs when $t_2/t_1 = 2$. Note that other curves could be fitted through data generated over incubation times of up to 48 h and could, in theory, be used equally well to estimate μ . For example, a curve could be required to pass through each of the diurnal maxima. Let the first maxima occur at time t_p (d) (the end of the first photoperiod); then the second maxima would occur 24 h later at time $1 + t_p$, which would lead to the exponent in Eq. 7 changing to $(1 + t_p)/t_p$. Because t_p is < 1 , this results in an exponent > 2 , which turns Eq. 7 into a higher order polynomial equation that is more difficult to solve. Therefore, restricting our exponent in Eq. 7 to be equal to 2 allows for an analytical solution for μ and forces the curve to pass through the 24-h minima.

Letting $t_2/t_1 = 2$ and solving Eq. 7 for C_{low}^* yields

$$C_{\text{low}}^* = \frac{C^*(t_1)^2}{2C^*(t_1) - C^*(t_2)}; \quad (8)$$

substituting back into Eq. 6, μ can be expressed as

$$\mu = \frac{-1}{t_1} \ln \left[1 - \frac{C^*(t_1)}{C_{\text{low}}^*} \right] \quad (9)$$

where t_1 is in days. In order for Eq. 9 to be correctly applied, recall that t_1 must be equal to 1 d and, correspondingly, $t_2 = 2$ d. Therefore, the effective daily growth rate, μ , calculated at $t_1 = 1$ d is

$$\mu = -\ln \left[1 - \frac{C^*(t_1 = 1 \text{ d})}{C_{\text{low}}^*} \right]. \quad (10)$$

In Eq. 10, $t_1 = 1$ d was substituted directly into the equation to emphasize the need for 24-h incubation. Equations 6–10 are called the diurnal model (DM) because the model requires data at 24 and 48 h.

To estimate μ from incubation times of 24 h or less, we start with the general solution to the VUDM and substitute the continuous division assumption (i.e. $\lambda_2 = 1$), making this a variable uptake-constant division model (VUCDM). If growth rates exceed 0.7 d^{-1} , most algal species will divide more than once per day. Therefore, as growth rates increase, so too must the division pattern appear more continuous in time and the more valid the VUCDM becomes. However, if the growth rate is low, the assumption of continuous division most likely cannot be met. The VUCDM is described as

$$C^*(t) = \alpha U \int_0^t \lambda_1(\tau) \exp[-\mu(t - \tau)] d\tau. \quad (11)$$

Before Eq. 11 can be solved, λ_1 must be specified. Let t_p equal the fraction of the day represented by light. Then the simplest useful expression for λ_1 is

$$\lambda_1(t) = \begin{cases} L_0 & nt_1 \leq t \leq nt_1 + t_p \\ 0 & nt_1 + t_p < t < (n+1)t_1, \quad n=0, 1, 2, \dots \end{cases} \quad (12)$$

L_0 is the weighted average of λ_1 over the light period t_p and is always ≤ 1 . The light period begins at 0 h and ends at t_p . When $L_0 = 1$, it represents the maximum rate of uptake of C^* ; it occurs whenever light intensity is at light saturation levels. Using $n = 0$ in Eq. 12, then substituting Eq. 12 into 11 and integrating over 24 h, t_1 , yields after simplification

$$C^*(t_1) = \frac{\alpha U}{\mu} L_0 [1 - \exp(-\mu t_p)] \exp[-\mu(t_1 - t_p)]. \quad (13)$$

It has been shown already in the CUDM that the maximum possible asymptotic concentration of C^* is m^*C_a . Substituting m^*C_a for $\alpha U/\mu$ in Eq. 13 gives us the final expression for determining μ from the VUCDM:

$$C^*(t_1) = m^*C_a L_0 [1 - \exp(-\mu t_p)] \exp[-\mu(t_1 - t_p)]. \quad (14a)$$

All of the terms in Eq. 14a can be determined from measurement except μ . When λ_1 can be represented in a simple manner, as in Eq. 12, then the VUCDM is directly integrable, giving an analytical expression for C^* . However, when the model is integrated over a 24-h period, the resulting expression is usually sufficiently nonlinear that further simplification is not possible, and μ must be solved for numerically, as seen in Eq. 14a. If incubations are restricted to the light period, μ can be solved for analytically. For example, following the same line of reasoning used in generating Eq. 14a but now applied to t_p renders a simplified version of Eq. 14a that can be directly solved for μ :

$$C^*(t_p) = m^*C_a L_0 [1 - \exp(-\mu t_p)] \quad (14b)$$

$$\mu = -\frac{1}{t_p} \ln \left[1 - \frac{C^*(t_p)}{m^*C_a L_0} \right]. \quad (14c)$$

Notice that the main difference between μ solved for in Eq. 14c and in the CUDM in Eq. 2 is that Eq. 14c explicitly includes the effect of variable uptake (L_0 in this simplified case) on the calculated μ value. In this example, whenever L_0 is < 1 , the μ value calculated by the VUCDM will always be greater than that calculated by the CUDM. This will only be true, however, provided that the asymptotic concentrations of C^* used in the CUDM and the VUCDM differ from each other in the same manner as described in these models.

Figure 3 illustrates how $C^*(t)$ is affected by high and low growth rates and by the nature of the division cycle. Curves A–D correspond to the various uptake and division cycles shown in Fig. 1a–d with the same 14:10 L/D cycle. The most obvious difference in Fig. 3 is between the exponential solutions from the CUDM and the other model solutions of cases A–D. Under low growth conditions (Fig. 3b), the time-course of C^* shows little sensitivity to the timing of the division cycle. However, as the growth or division rate increases (Fig. 3a), clear differences in C^* emerge. The maximum 24-h C^* occurs

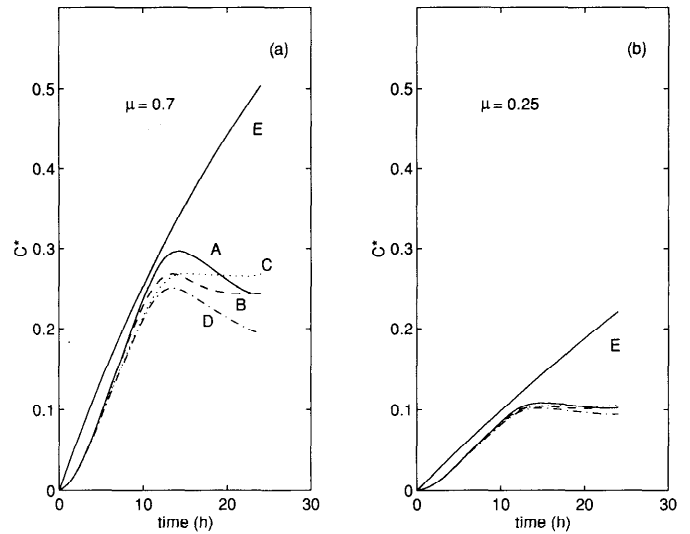


Fig. 3. The effect of high (a) and low (b) growth rates and growth cycle on C^* . Curves A–D correspond to the carbon uptake and growth cycles in Fig. 1a–d. Curves A–C were generated by the variable uptake-division model and curve D by the continuous division model. Curve E shows C^* as calculated by the constant uptake-division model with μ values of 0.7 and 0.25 d^{-1} .

when division is restricted to the light cycle (curve C), and the minimum 24-h C^* occurs when division is continuous throughout the day (curve D).

During the course of the daily L/D cycle, each curve will peak near the end of the 14-h light cycle. At this time, the C^* concentration with the highest peak occurs when cell division is concentrated during the dark cycle (curve A). Conversely, when algal division rates can be represented as a continuous process via the VUCDM (curve D), the peak C^* will be smaller than that seen in the other cases. It is important to note that all of these errors are small relative to the errors associated with the CUDM (curve E) if it is blindly applied to both the light and dark cycle.

None of this is surprising, because at the cellular level division represents the only loss mechanism for C^* that is accounted for by any of these models. Hence, the longer this mechanism operates in time or the more it directly operates during the light cycle (curves B and C), the more effective division becomes at limiting C^* . Furthermore, the effect of light (or more exactly, variable uptake) on C^* is clearly evident in Fig. 3. Notice how during the photoperiod curves A–D under both low and high growth rates show C^* increasing at a rate slower than that seen in curve E under the CUDM. The cause is the way $\lambda_1(t)$ is described. In this case, the prescribed values of $\lambda_1(t)$ were chosen to mimic a time-course of light levels that allows the maximum rate of uptake for only a couple of hours during the photoperiod (Fig. 1). In contrast, the CUDM uptake rate progresses at its maximum throughout the entire photoperiod. The net consequence is that exponential fits to data based on the CUDM, even if applied only to data generated during the photoperiod,

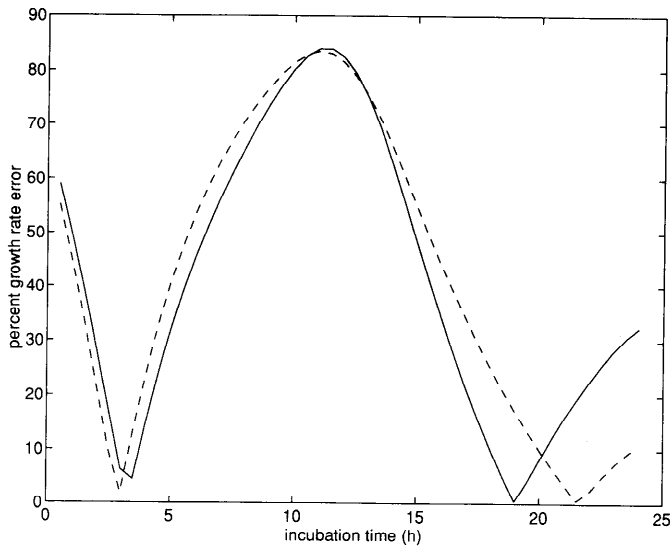


Fig. 4. Percentage error in effective daily μ values vs. incubation time if the constant uptake-division model is used to describe curve D in Fig. 3. The solid line corresponds to high growth rates ($\mu = 0.7 \text{ d}^{-1}$), and the dashed line corresponds to low growth rates ($\mu = 0.25 \text{ d}^{-1}$).

will underestimate the true μ if variable uptake conditions exist and the wrong asymptotic estimate of C^* is used. A mathematical example using the VUCDM demonstrates in Eq. 14c how variable uptake conditions may impact μ estimates.

Another concern that further compounds the difficulty of making accurate estimates of μ occurs when the CUDM is applied to data with variable incubation times. For example, Fig. 4 shows the percentage growth rate error vs. incubation time that occurs when the CUDM is used to estimate μ from the artificial data shown in Fig. 3 (case D, VUCDM). The correct μ is 0.7 and 0.25 d^{-1} , and it is exactly recovered by the DM using only 24- and 48-h data. However, if the CUDM is used, the average error in μ is 40% for all incubations from 1 to 24 h long for both high (solid line, Fig. 4) and low (dashed line, Fig. 4) division rates. The error reaches a maximum of $>80\%$ near the 12-h incubation times for both high and low growth rates. Minimum errors of near 0% occur at times near 5 and 20 h. These minima and the error curves will change with different photoperiods, which illustrates the potential for inaccurate μ values calculated with the CUDM.

The 48-h incubation time required to calculate μ by the DM avoids the difficulty of making a priori estimate of C^*_{low} by directly solving for C^*_{low} from measurements of C^* at 24 and 48 h. This is the major drawback to the DM, because incubations must be done in containers large enough that problems due to containment effects are minimized. As will be seen later in the data example, the calculated μ values are very sensitive to the 24- and 48-h C^* values. Furthermore, practical concerns suggest that 48-h incubations are unlikely to be widely used because of the demands that would place on

limited resources. Simpler than the VUDM and without the requirement of the 48-h incubation times of the DM is to estimate μ from the VUCDM.

The relationship between the DM and the VUCDM can be seen by describing λ_1 according to Eq. 12 and examining the asymptotic behavior of C^* . If Eq. 12 is substituted into the VUCDM (Eq. 11) and integrated over several days, the result can be generalized into a series solution for C^* :

$$C^*(t_n) = m^*C_aL_0[1 - \exp(-\mu t_p)] \cdot \sum_{j=1}^n \exp[-\mu(jt_1 - t_p)]. \quad (15)$$

The summation term in Eq. 15 represents the net effect of dark division, $\mu(t_1 - t_p)$, on reducing the maximum possible C^* (C^*_{high}) to its lower asymptotic value (C^*_{low}). As n grows very large, the asymptotic value of $C^*(t_n)$ equals C^*_{low} used in the DM. Equation 15 can be algebraically simplified so that C^*_{low} , according to this application of the VUCDM, can be expressed as

$$C^*_{\text{low}} = m^*C_aL_0 \left[\frac{1 - \exp(-\mu t_p)}{1 - \exp(-\mu t_1)} \right] \exp[-\mu(t_1 - t_p)]. \quad (16)$$

The diurnal maxima in C^* according to the VUCDM occur at t_p . If a similar line of reasoning is used to derive C^*_{high} , as was used above in deriving an expression for C^*_{low} , it can be shown that

$$C^*_{\text{high}} = m^*C_aL_0 \left[\frac{1 - \exp(-\mu t_p)}{1 - \exp(-\mu t_1)} \right]. \quad (17)$$

Notice the direct manner by which L_0 and the duration of the dark period ($t_1 - t_p$) affect the magnitude of the asymptotic concentrations of C^* in Eq. 16 and 17. The relationship between C^*_{low} and C^*_{high} is more clear if Eq. 17 is substituted into 16:

$$C^*_{\text{low}} = C^*_{\text{high}} \exp[-\mu(t_1 - t_p)]. \quad (18)$$

As the duration of the dark period decreases, so does the difference between the upper and lower asymptotes of C^* . Obviously, under continuous light conditions there will be only one asymptotic value for C^* equal to $m^*C_aL_0$, which has already been seen and discussed.

Although the VUCDM is a better descriptor of algal processes than the DM is, care must still be exercised in applying this model. We use the analytical solution of the VUCDM in Eq. 14a to illustrate this problem. From a single measurement of C^* taken at the end of a 24-h incubation time, t_1 , there may be two different values of μ that exactly satisfy Eq. 14a. Thus, a critical μ value exists, μ_{crit} , for all photoperiods that are less than continuous. The major concern over μ_{crit} occurs when it falls within the realm of possible division rates that one might calculate from data. We find the dependency of μ_{crit} on t_p by differentiating Eq. 14a with respect to μ and setting it equal to zero. If this is done, then

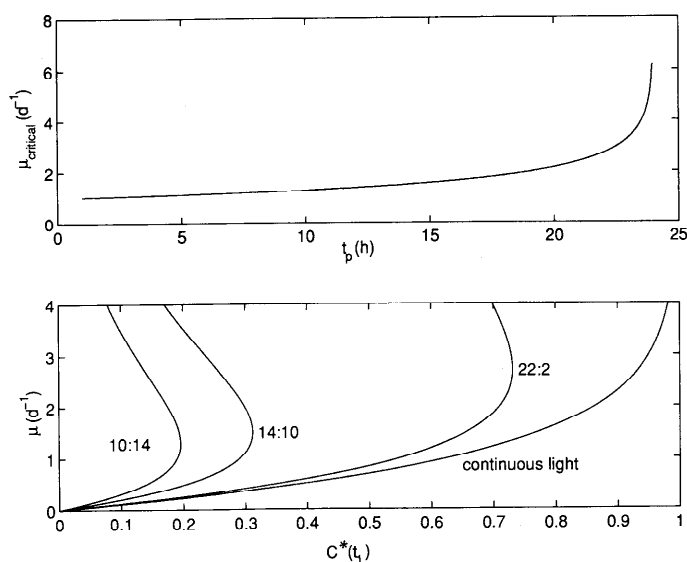


Fig. 5. Top half of figure is a graph of Eq. 19 and shows how μ_{crit} depends on t_p . The bottom half of the figure plots μ vs. $C^*(t_i)$, where μ is calculated from four different values of the L/D cycle and the continuous division model solution shown in Eq. 14a.

$$\mu_{\text{crit}} = \frac{1}{t_p} \ln \left[\frac{1}{1 - t_p} \right]. \quad (19)$$

The top half of Fig. 5 is a graph of μ_{crit} vs. t_p for t_p ranging from 1 h to near 24 h. Even when the dark period is relatively brief, μ_{crit} drops from large values fast enough that it cannot be ignored [e.g. 22:2 L/D period has a μ_{crit} of 2.7 (d^{-1})]. What this and the bottom half of Fig. 5 suggest is that μ cannot be uniquely determined with the VUCDM and a single measurement of C^* at 24 h. For example, if C^* at the end of 24 h is equal to 0.25 $m^*C_aL_0$ and the L/D period is 14:10, then from the bottom half of Fig. 5, we see that there are two values of μ , ~ 0.7 and 2.8 d^{-1} , that satisfy Eq. 14a. In most cases, the two values of μ are so different that one can easily be eliminated, particularly if there is some information about the possible range of growth for that particular system. For example, in most cases the high second value of μ will be close to or exceed 2 d^{-1} (Fig. 5), and growth rates of this magnitude are rare in both freshwater and marine systems (Reynolds 1984; Furnas 1990). However, if necessary, this ambiguity in uniquely determining μ can be resolved by making an additional measurement of C^* at some time during the 24-h incubation, such as near the end of the photoperiod. Integrating the VUCDM for the two sample times will thus provide a means to determine μ uniquely. However, for analyses in which C^* is restricted to the photoperiod, μ can be directly calculated as in Eq. 14b and 14c.

We use data from Knoechel and Quinn (1989) to demonstrate how these models are applied to data. It is not our purpose to reinterpret their results but rather to use their data as an illustrative example. To be consistent with their observations, C^* will represent the new cell

Table 1. Log-phase culture data from Knoechel and Quinn 1989.

| Time (h) | C^* (pg C cell $^{-1}$) | Time (h) | C^* (pg C cell $^{-1}$) |
|----------|----------------------------|----------|----------------------------|
| 0 | 0.27 | 24.5 | 5.04 |
| 0.5 | 0.47 | 26.5 | 5.43 |
| 2.5 | 0.79 | 28.5 | 6.09 |
| 4.5 | 1.22 | 30.5 | 6.50 |
| 6.5 | 2.16 | 32.5 | 6.47 |
| 8.5 | 3.46 | 34.5 | 8.18 |
| 10.5 | 3.76 | 36.5 | 6.15 |
| 12.5 | 4.38 | 38.5 | 6.90 |
| 14.5 | 6.98 | 39.5 | 8.83 |
| 15.8 | 7.87 | 41.5 | 8.34 |
| 18.5 | 5.97 | 43.5 | 5.86 |
| 20.5 | 6.46 | 45.5 | 6.10 |
| 22.5 | 6.42 | 47.5 | 8.29 |
| 23.7 | 4.65 | | |

carbon concentration with units of pg C cell $^{-1}$. Correspondingly, the uptake rate parameter, U , used by the models will now represent the rate at which new cell carbon is produced.

Table 1 lists the first 48 h of data corresponding to Knoechel and Quinn's figure 7. They used the CUDM and applied it in a least-squares sense to data generated during light periods. They obtained a growth rate on the order of 0.5 d^{-1} depending on which estimate of the asymptotic C^* they used. We will not repeat this calculation.

The DM results yielded growth rates of 0.25 and 1.16 d^{-1} . This large difference in μ was calculated by using data at 23.7 and 45.5 h for the high μ , and the low μ was calculated from the 23.7- and 47.5-h data. Although there is much scatter in the data, the results demonstrate that if the DM is used to estimate μ , the level of uncertainty in C^* must be known before any confidence can be placed on the μ estimate.

Figure 6 and Table 2 show the results of the VUDM and the VUCDM applications. The previously described methods for estimating the asymptotic C^* are not applicable in this example, so we chose two values based on Knoechel and Quinn's (1989) approach. In Fig. 6a, an asymptotic C^* of 11.8 pg C cell $^{-1}$ was used, corresponding to a maximum cell carbon based on the assumption that the maximum is 10% of the mass: volume ratio of the algal species under study. For the algal cells in log phase, cell volume ranged from 100 to 150 μm^3 . A higher maximum of cell carbon of 25 pg C cell $^{-1}$ was used in Fig. 6b. This value was chosen based on the same assumptions as in Fig. 6a, except a larger cell volume (250 μm^3) was assumed, which corresponds to the smaller cells in the stationary growth phase (250–400 μm^3 , Knoechel and Quinn 1989). Table 2 lists the model results, with cases a–c representing the VUDM and case d representing the VUCDM. Cases a–d represent the different division patterns seen in Fig. 1a–d, with a = dark division, b = light/dark division, c = light division, and d = continuous division.

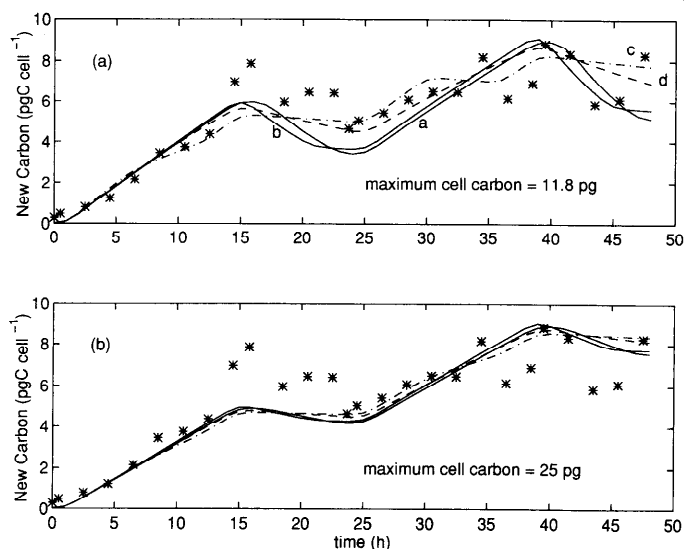


Fig. 6. Plot of data (*) against optimal model solutions when maximum cell carbon content is 11.8 and 25 pg. In panel a, curves a–c correspond to the variable uptake-division model and curve d represents the continuous division model. In panel b, all four curves track similarly.

Our procedure to apply the models follows. First, we determine the maximum possible C^* , second, we determine $\lambda_1(t)$ and $\lambda_2(t)$. We used a 16 : 8 L/D cycle. To simplify model application, we set $\lambda_1(t)$ equal to one over hours 2–14 and then linearly decreased it to zero at hours 0 and 16. We used identical treatment to describe $\lambda_2(t)$ over the 8-h time that it was operational. $\lambda_2(t)$ was linearly ramped up from zero to one over the first 2 h, and then linearly ramped down from one to zero over the last 2 h and held constant in between at one. Specifically, $\lambda_2(t)$ for case a was restricted to the dark period, for case b it operated for the last 4 h of the light period and the first 4 h of the dark, and for case c it operated for 8 h in the light period only. Third, we numerically calculate hourly values of C^* according to the two models by using a broad range of μ values. In these cases, we let μ range from 0.1 to 2.5 d^{-1} in increments of 0.02. We carried out the integration until the change in the daily peak C^* , $C^*(t_p)$, from one day to the next was $<1\%$ or until 2 weeks passed, whichever came first. At lower values of μ , the maximum C^* may not be achieved in a 2-week-long integration because of slow convergence. However, the error induced by this will have little effect on the results. Fourth, we scale C^* over the period for which observations of interest exist by multiplying the calculated C^* values by the ratio of estimated asymptotic C^* based on data to the calculated asymptotic C^* from the model. Finally, we calculate goodness-of-fit between modeled C^* and data by calculating the root-mean-square (rms) error or by using some other measure. In this example, the optimal μ gives the lowest rms error.

Figure 6 shows considerable scatter in the data beginning about 12 h after the experiment starts. Each of the optimal trajectories describes the data best during this

Table 2. Model results. Cases a–c correspond to the variable uptake-division model and case d corresponds to the variable uptake-constant division model.

| Case | Calculated μ (d^{-1}) | Asymptotic C^* | rms error |
|------|----------------------------------|------------------|-----------|
| a | 2.18 | 11.8 | 0.26 |
| b | 2.02 | 11.8 | 0.27 |
| c | 1.84 | 11.8 | 0.20 |
| d | 0.64 | 11.8 | 0.20 |
| a | 0.64 | 25.0 | 0.25 |
| b | 0.66 | 25.0 | 0.24 |
| c | 0.62 | 25.0 | 0.25 |
| d | 0.20 | 25.0 | 0.25 |

period, and each curve in both Fig. 6a and b has similar rms error of ~ 0.25 pg C cell $^{-1}$ (Table 2). The results also show the μ estimates to be sensitive to the asymptotic C^* used in the calculation, the duration of the L/D cycle, and whether division can be considered to be continuous. Note that because of the way the asymptotic C^* has been applied in this example, the results are not sensitive to the phasing of the division cycle with respect to the light cycle. Given what we do know about the data (i.e. that 25 pg C cell $^{-1}$ is a more reasonable estimate of the maximum C^* than 11.8 pg C cell $^{-1}$ is) and that division is discontinuous in time (Knoechel and Quinn 1989), the μ values calculated with the VUDM (~ 0.6 d^{-1}) seem to be the best growth rate estimates. This growth rate from the VUDM is very similar to the growth rate determined from changes in cell density during the first day of the ^{14}C experiment (Knoechel and Quinn 1989).

Four points are concluded. First, μ estimates based on the CUDM are only applicable for describing C^* and algal growth rates under continuous light and division conditions. The application of μ estimates based on the CUDM to daily growth rates with both light and dark periods will subject the application to possibly large errors because of the violation of the critical model assumption of continuous light and carbon uptake; furthermore, μ values calculated in this manner will change under photoperiods of different duration. Second, the VUDM can accurately represent algal processes and provide robust μ estimates, but the model has increased data needs which include information on the algal division pattern for each species under study. Third, the DM can also provide accurate μ estimates while requiring only two measurements of C^* and no other parameters, but it requires 48-h incubation times; although the DM describes C^* as an exponential curve, as does the CUDM, it will nonetheless generate a μ value identical to that of the continuous division model that passes through the same points. Finally, the VUCDM can also render accurate μ estimates, but it requires estimates of m^* , C_a , $\lambda_1(t)$, and t_p as well as at least one measurement of C^* . Although this model and the VUDM demand additional work compared to the CUDM, the effort is warranted because they provide a direct approach for quantifying the dependence of μ on the photoperiod

and thus enable greater confidence in applying μ to different environmental conditions.

Michael J. McCormick

NOAA
Great Lakes Environmental Research Laboratory
2205 Commonwealth Blvd.
Ann Arbor, Michigan 48105

Gary L. Fahnenstiel

NOAA
Lake Michigan Field Station
1431 Beach St.
Muskegon, Michigan 49441

*Steven E. Lohrenz
Donald G. Redalje*

Center for Marine Science
University of Southern Mississippi
Stennis Space Center 39529

References

- CHISHOLM, S. W. 1981. Temporal patterns of cell division in unicellular algae, p. 150–181. *In* Physiological bases of phytoplankton ecology. Can. Bull. Fish. Aquat. Sci. 210.
- FAHNENSTIEL, G. L., AND D. SCAVIA. 1987. Dynamics of Lake Michigan phytoplankton: Primary production and growth. Can. J. Fish. Aquat. Sci. 44: 499–508.
- FURNAS, M. J. 1990. In situ growth rates of marine phytoplankton: Approaches to measurement, community and species growth rates. J. Plankton Res. 12: 1117–1151.
- HARRIS, G. P. 1978. Photosynthesis, productivity and growth: The physiological ecology of phytoplankton. *Ergeb. Limnol.* 10: 171 p.
- KNOEHEL, R., AND J. KALFF. 1975. Algal sedimentation: The cause of a diatom-blue-green succession. *Int. Ver. Theor. Angew. Limnol. Verh.* 19: 745–754.
- , AND ———. 1976. Track autoradiography, a method for the determination of phytoplankton species productivity. *Limnol. Oceanogr.* 21: 590–596.
- , AND ———. 1978. An in situ study of the productivity and population dynamics of five freshwater planktonic diatom species. *Limnol. Oceanogr.* 23: 195–218.
- , AND E. M. QUINN. 1989. Carbon dynamics of logarithmic and stationary phase phytoplankton as determined by track autoradiography. *Cytometry* 10: 612–621.
- LAWS, E. A., G. R. DiTULLIO, AND D. G. REDALJE. 1987. High phytoplankton growth and production rates in the North Pacific subtropical gyre. *Limnol. Oceanogr.* 32: 905–918.
- LI, W. K. W. 1994. Primary production of prochlorophytes, cyanobacteria, and eucaryotic ultraphytoplankton: Measurements from flow cytometric sorting. *Limnol. Oceanogr.* 39: 169–175.
- MINGELBIER, M., B. KLEIN, M. R. CLAERBOUDT, AND L. LEGENDRE. 1994. Measurement of daily primary production using 24 h incubations with the ^{14}C method: A caveat. *Mar. Ecol. Prog. Ser.* 113: 301–309.
- REYNOLDS, C. S. 1984. The ecology of freshwater phytoplankton. Cambridge.
- RIVKIN, R. B., D. A. PHINNEY, AND C. M. YENTSCH. 1986. Effects of flow cytometric analysis and cell sorting on photosynthetic carbon uptake by phytoplankton in cultures and from natural populations. *Appl. Environ. Microbiol.* 52: 935–938.
- , AND H. H. SELIGER. 1981. Liquid scintillation counting for ^{14}C uptake of single algal cells isolated from natural samples. *Limnol. Oceanogr.* 26: 780–785.
- SODER, C. J. 1966. Some aspects of phytoplankton growth and activity, p. 47–59. *In* C. R. Goldman [ed.], Primary productivity in aquatic environments. Univ. California.
- SUBBA RAO, D. V. 1988. Species-specific primary production measurements of Arctic phytoplankton. *Br. Phycol. J.* 23: 273–282.
- WELSCHMEYER, N. A., R. GOERICKE, S. STROM, AND W. PETERSON. 1991. Phytoplankton growth and herbivory in the subarctic Pacific: A chemotaxonomic analysis. *Limnol. Oceanogr.* 36: 1631–1649.
- , AND C. J. LORENZEN. 1984. Carbon-14 labeling of phytoplankton carbon and chlorophyll *a* carbon: Determination of specific growth rates. *Limnol. Oceanogr.* 29: 135–145.

Acknowledgments

We thank Ray Knoechel for supplying us with data to demonstrate the model applications. We also thank Paul Liu of GLERL for his mathematical insights.

This work was partially supported by the Nutrient Enhanced Coastal Ocean Productivity program of NOAA. GLERL Contribution 919.

*Submitted: 25 July 1994
Accepted: 13 June 1995
Amended: 26 September 1995*